Available online at www.sciencedirect.com
SCIENCE DIRECT®
Journal of Chromatography A, 1033 (2004) 311–319
JOURNAL OF CHROMATOGRAPHY A
www.elsevier.com/locate/chroma

Quantitative magnetic resonance imaging of urea and lysozyme in protein chromatography

D.J. Holland, A.J. Sederman, M.D. Mantle, L.F. Gladden*, A.P.J. Middelberg

Department of Chemical Engineering, University of Cambridge, Pembroke Street, Cambridge CB2 3RA, UK

Received 29 August 2003; received in revised form 6 January 2004; accepted 9 January 2004

Abstract

Magnetic resonance imaging (MRI) techniques have been implemented to enable quantitative imaging of protein and urea within a 5 ml HiTrap size-exclusion chromatography desalting column, without introduction of contrast agents. One-, two- and three-dimensional images of urea injected at concentrations of 2, 4, 6 and 8 M were acquired. One-dimensional profiles of lysozyme at concentrations between 5 and 25 mg ml^{-1} were also obtained. All data were accurate to within ±15% when compared to the known amount injected. Quantitative MRI elution profiles of both urea and lysozyme were then obtained in real-time during a desalting separation.

Keywords: Magnetic resonance imaging; Nuclear magnetic resonance; Urea; Lysozyme; Proteins

1. Introduction

Size-exclusion chromatography (SEC) uses a packed bed of porous particles to separate molecules of different sizes. Common applications of SEC include removal of buffer salts after refolding of proteins, size-based separation of biomolecules, and as a method to determine molecular weights and molecular weight distributions of polymers. The quality of the separation achieved using SEC is very dependent on the flow profile throughout the bed, the sample distribution across the top of the bed and on the quality of the bed packing [1]. In order to quantify the effect of these and other parameters on the observed elution profile characterising a column it is desirable to directly visualise and quantify sample movement through the packed bed.

Magnetic resonance (MR) imaging provides a means of non-invasively monitoring chromatographic separations [2]. In order to produce suitable contrast in the MR images, the sample to be eluted is commonly doped with a paramagnetic tracer ion such as gadolinium. Plante et al. [2] obtained qualitative images of viscous fingering of bovine serum albumin (BSA) samples within a column at concentrations as low as 30 mg ml^{-1} by labelling BSA with gadolinium. However, although this provides a means of qualitatively investigating the elution profile in a column, quantitative analysis is complicated by the labelling process due to uncertainty of the uniformity of labelling and the effect of the label on the nuclear spin relaxation parameters and hence the resulting contrast within the MR image. This final point has been considered by earlier workers. For example, Tallarek et al. [3] examined how the MR signal intensity varies as a function of gadolinium concentration. Gadolinium was found to alter both the spin–lattice (T_1) and spin–spin (T_2) relaxation times of surrounding water molecules such that signal intensity is a very nonlinear function of gadolinium concentration, reaching a maximum at 1 mM. To minimise the ambiguity in interpreting the signal intensity, all images reported by Tallarek et al. [3] were recorded under conditions such that the gadolinium concentration within the column was less than 1 mM. Mitchell et al. [4] used a similar approach to obtain quantitative images of Gd-DTPA by keeping the gadolinium concentration below 2.5 mM. In order to validate the calibration of gadolinium, height equivalent to a theoretical plate (HETP) values were calculated from the peak-width at half height and were of the order of 100 μm for the well-packed columns. These were found to increase linearly along the length of the column as expected for a homogeneously packed column without extra-column band broadening. The HETP values measured using MR were found to be comparable to those

* Corresponding author. Tel.: +44-1223-334777; fax: +44-1223-334796.
E-mail address: gladden@cheng.cam.ac.uk (L.F. Gladden).

0021-9673/$ – see front matter © 2004 Elsevier B.V. All rights reserved.
doi:10.1016/j.chroma.2004.01.016

obtained chromatographically [4]. Mitchell et al. [4] were also able to image a size-based protein separation of BSA and chymotrypsinogen A by labelling both proteins with gadolinium.

In addition to the uses of SEC described above, since 1986 work has begun on examining the viability of chromatography as a means of refolding proteins. Recombinant human ETS-1 protein and bovine ribonuclease A have been successfully refolded using a size-exclusion matrix [5]. In some cases, SEC has been shown to result in an increased yield of native protein over batch dilution. It has been proposed that as the protein folds the associated decrease in hydrodynamic radius permits greater access into the pores of the gel matrix. Transport of the protein within the pores is then diffusion dominated and consequently protein–protein collisions are less likely, therefore limiting aggregation [6]. However, an equally important factor may be the method of removal of reducing agents [7,8] and denaturant [9,10] characteristic of an SEC-based process. Therefore, as well as providing insight into column design and modelling of SEC, direct visualisation of the changing chemical environment experienced by a protein inside an SEC column may clarify the mechanism of protein refolding using SEC.

In this work, two sets of experiments are reported. First, quantitative three-dimensional ^{1}H images of a pulse of urea moving through the column are shown. Prior to the experiment, a calibration plot of urea concentration versus ^{1}H signal intensity was obtained such that quantitative urea concentrations within the column are obtained directly from the ^{1}H signal intensities associated with each voxel in the three-dimensional MR image. The quantitative nature of the MR measurement was confirmed by comparing the total urea content in the column determined using MR with the known amount injected into the column. One-dimensional concentration profiles of urea along the length of the column were also compared with standard chromatographic elution profiles.

Second, a method for obtaining one-dimensional ^{1}H concentration profiles of unlabelled lysozyme is reported. Quantitative lysozyme concentration profiles are obtained from these data. This approach is then used to acquire time-resolved urea and lysozyme concentration profiles within the column, in real-time, during a desalting process.

2. Theory

The relevant theory of MR techniques is well documented [11,12] and is not reproduced here. However, to acquire the quantitative measurements of concentration presented, it is important to understand the effects of nuclear spin relaxation time contrast on the acquired signal, for the particular magnetic resonance radiofrequency (RF) pulse sequences used.

In the MR experiment, an RF excitation is applied to the nuclear spin system which, at equilibrium, is characterised by a net magnetisation vector, M_0, aligned along the direction of the static magnetic field B_0; this direction is conventionally taken to be z. The RF pulse causes the net magnetisation to rotate into the x–y plane, and the return of the system to equilibrium is then recorded, in the form of a decaying, oscillatory RF signal detected in a receiver coil placed around the sample. The return of the system to equilibrium is characterised by two processes known as spin–lattice (T_1) and spin–spin (T_2) relaxation. For a spin-echo [13] pulse sequence, the decaying magnetisation in the x–y plane is described by [11]:

$$M_{xy} = M_0 \left[1 + \exp\left(-\frac{T_R}{T_1}\right)\right] \exp\left(-\frac{2T_E}{T_2}\right), \quad (1)$$

where T_R is the time between successive repetitions of the RF pulse sequence. The acquired signal is commonly referred to as an 'echo'.

Eq. (1) assumes that the RF pulses are perfect 90 and 180° pulses, respectively, and that the echo time, T_E, is much less than both T_1 and T_R. For a spin-echo sequence with multiple echo detection [14], the echo amplitude (i.e. signal intensity) for any echo, n, will be governed by:

$$M_{xy} = M_0 \left[1 - \exp\left(-\frac{T_R - (2N-1)T_E/2}{T_1}\right)\right] \times \exp\left(-\frac{nT_E}{T_2}\right), \quad (2)$$

where N is the total number of echoes in the train.

T_1 relaxation was also exploited in this work to discriminate between a species of interest (e.g. urea) and any background signal associated with the buffer solution. The equation describing the recovery of the magnetisation along the z-direction following RF excitation is of the form:

$$M_z(t) = M_z(0) \exp\left(-\frac{t}{T_1}\right) + M_0 \left(1 - \exp\left(-\frac{t}{T_1}\right)\right). \quad (3)$$

It follows from Eq. (3) that if the two components of interest are characterised by significantly different T_1 relaxation times, it is possible to selectively suppress the signal from the component which is not of interest. Let us assume that we wish to discriminate species A and B; and that species A is of interest. To achieve this, an RF excitation which inverts the magnetisation (i.e. a 180° pulse) is applied. By acquiring signal at a time $0.6931T_1$(B) after this RF excitation pulse was applied, suppression of the signal from B is achieved and the dominant contribution to the acquired signal is associated with species A. If this inversion recovery pulse is used Eqs. (1) and (2) can be modified as follows:

$$M_{xy} = M_0 \left[1 - 2\exp\left(-\frac{T_I}{T_1}\right) + \exp\left(-\frac{T_R}{T_1}\right)\right] \times \exp\left(-\frac{2T_E}{T_2}\right) \quad (4)$$

$$M_{xy} = M_0 \left[1 - 2\exp\left(-\frac{T_I}{T_1}\right) \times -\exp\left(-\frac{T_R - (2N-1)T_E/2}{T_1}\right)\right] \exp\left(-\frac{nT_E}{T_2}\right) \quad (5)$$

where T_I is the time delay between the initial 180° excitation pulse and the start of data acquisition.

The RF pulse sequences used in this paper were all based on a standard spin-echo sequence with multiple echo collection. Employing this experimental methodology achieved both reduced acquisition times and increased T_2 weighting in the data. In order to capture two- and three-dimensional images, a rapid acquisition with relaxation enhancement (RARE) fast imaging sequence based on that proposed by Hennig et al. [15], was incorporated into the echo train. The actual RARE imaging sequence used was that developed by Sederman et al. [16]. Similarly, one-dimensional profiles were recorded using multiple echoes. As stated above, the implementation of multiple echoes will increase the T_2 weighting of the resulting profile (see Eq. (5)) and the signal-to-noise ratio in the data. These two effects can be further optimised by selective echo collection; if the first few echoes are discarded the signal-to-noise will be lower, but the T_2 weighting will be enhanced. The effect of this is that the contrast level in the image is enhanced and hence the effective signal-to-noise ratio in the image increases. A further increase in signal-to-noise is achieved if no read gradients are applied during the echoes that are not collected, thereby reducing the effect of diffusion (i.e. signal attenuation) in the acquired data [11].

3. Experimental

3.1. Chemicals

Urea, dithiothreitol (DTT), hen egg white lysozyme, monobasic potassium phosphate (NaH_2PO_4) and dibasic potassium phosphate (Na_2HPO_4) were purchased from Sigma (Dorset, UK). The buffer solution used was 20 mM phosphate buffer at pH 7.0.

3.2. Chromatography

The studies were carried out using a 5 ml HiTrap desalting column (Amersham Biosciences UK, Bucks, UK). The column was prepacked with a Sephadex G-25 Superfine matrix, which is based on cross-linked dextran beads. The bead size was 15–70 μm with an exclusion limit of 5000 Da.

For the MR imaging experiments, samples were loaded onto the column using a six-port Rheodyne sampling valve with a 500 μl sample loop. Approximately 2 m of 0.8 mm i.d. polyethylene tubing was required to connect the valve to the column. The length of tubing used causes some extra-column pulse broadening, estimated to be ~0.75 mm once the pulse has entered the column. A Pharmacia fast-protein liquid chromatography (FPLC) P-500 syringe pump was used to deliver the buffer solution. The flow rate used for all experiments, unless otherwise specified, was 0.5 ml min^{-1}, giving a superficial linear velocity of 2.5 mm min^{-1} and a *Pe* number (based on the column length) of approximately 500.

To determine the calibration plot for urea concentration, a column equilibrated with an appropriate concentration of urea was imaged using the same imaging sequence as that used in the imaging of the elution of 0.5 ml samples of urea.

For the conventional chromatography experiments, samples were loaded onto the column using a seven-port Rheodyne sampling valve with a 500 μl sample loop. Approximately 0.1 m of 0.8 mm i.d. polyethylene tubing was used to connect the sampling valve to the top of the column. Chromatographic elution profiles were recorded using an LKB Bromma 2210 two-channel data recorder connected to an Amersham Pharmacia Biotech UPC-900 UV and conductivity detector.

3.3. Magnetic resonance imaging

One-dimensional urea profiles were acquired using a standard profiling pulse sequence with a pre-conditioning inversion recovery pulse. One-dimensional lysozyme profiles were acquired using a profiling pulse sequence with multiple spin echoes as shown in Fig. 1. Two- and three-dimensional urea images were acquired using a RARE imaging sequence with a preconditioning inversion recovery pulse.

All MR images were obtained on a Bruker DMX 300 spectrometer equipped with a 25 mm diameter birdcage microimaging coil (transmitter/receiver coil effective length approximately 50 mm) operating at a ^1H frequency of 300.13 MHz. The HiTrap column was positioned vertically in the RF coil such that the centre of the column was in the centre of the RF coil. Spatial resolution was achieved using a three-axis shielded gradient system, with maximum gradient strengths in the *x*-, *y*- and *z*-directions of 0.96, 0.96 and 0.97 T m^{-1}, respectively. A brief description of the imaging protocol is given here.

The three-dimensional RARE imaging sequence was a standard slice-selective excitation with a preconditioning inversion recovery pulse and is referred to as a RARE IR RF

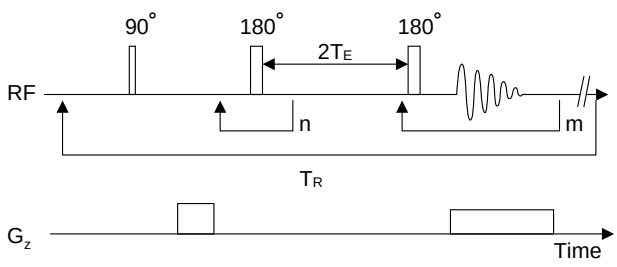

Fig. 1. Pulse sequence for one-dimensional lysozyme imaging, $n = 8$ and $m = 16$ for all lysozyme data shown.

pulse sequence. The inversion recovery delay (T_I) was 1 s, the recycle time (T_R) was 4 s, and 16 echoes were collected in each train. A data matrix of 128 × 64 × 64 was acquired in a total acquisition time of approximately 18 min. The field-of-view of each image was 40 mm × 20 mm × 20 mm, thus giving cubic image voxels and an inherent voxel resolution of 312 μm × 312 μm × 312 μm. In order to minimise motional distortion in the imaging of urea pulses, all three-dimensional images were acquired with no flow of buffer, i.e. flow to the column was stopped during image acquisition. Therefore, any distortion of the pulse within the image is due to diffusion only and is estimated to be less than 1 mm.

Two-dimensional RARE images were acquired using a two-dimensional RARE IR sequence. A 2 mm thick slice down the centre of the column was imaged using a RARE factor of 16. The field-of-view for the images was 40 mm × 20 mm, giving square voxels 312 μm × 312 μm. The total acquisition time was 37 s. One-dimensional profiles of urea in the column were obtained using a standard profiling sequence with the same preconditioning inversion pulse as was used in acquiring the RARE images. Profiles were recorded in the *z*-direction (i.e. along the length of the column) with a spatial resolution of 312 μm. Two scans were acquired giving a total acquisition time of 15 s.

One-dimensional profiles of lysozyme in the column were acquired using a conventional profiling sequence with multiple echo acquisition, as shown in Fig. 1. The first eight echoes were discarded and the next 16 were collected. This provides enhanced T_2 contrast with minimal loss in signal and minimal diffusion weighting. It also minimises the effect of unbalanced stimulated and spin echoes produced from imperfections in the RF pulses, and thus provides a more homogeneous profile. The field-of-view for these experiments was 50 mm. The stimulated and spin echoes were acquired separately, each consisting of 256 data points and then subsequently summed to produce a final profile with a data matrix of 256 to give a spatial resolution of 195 μm. Two experiments were performed with a repetition time of 7 s, giving a total acquisition time of 14 s.

Finally, the acquired data were Fourier transformed and then exported to a Linux-based workstation for further analysis using software available in the laboratory.

4. Results

4.1. Quantitative measurement of urea concentration

This section reports the use of MR imaging for quantitative analysis of urea distribution in a desalting column. First, the RARE IR imaging sequence is validated as a quantitative measure of urea concentration in a 5 ml HiTrap desalting column. Second, two-dimensional images, both extracted from the three-dimensional dataset and measured directly, clearly identify the spatial heterogeneity in transport of urea down the column.

Three-dimensional RARE IR images were acquired for a column equilibrated with urea in 20 mM phosphate buffer at pH 7.0. Four experiments were performed each with a different urea concentration: 2, 4, 6 and 8 M urea concentrations were used. The images were then analysed to determine the signal intensity per pixel by first normalising each image using a separate reference image of the column. Normalisation to a reference image allows any image artefacts arising from heterogeneity in receiver coil response and imperfections in the RF pulses to be removed prior to subsequent analysis. The reference image was recorded for a concentration of 8 M urea within the column. In each of the resulting images, the signal intensity from the central region of the column was averaged, i.e. all voxels which contained interfaces of the column packing with either the column wall or the entrance/exit to the column, were excluded from the analysis. This averaged normalised signal intensity was found to vary linearly with urea concentration. A calibration function for urea concentration against MR signal intensity was then produced and is given by Eq. (6):

$$[\text{Urea}] = 8.6S - 0.2 \quad (6)$$

where [Urea] is the concentration of urea (M) and S is the signal intensity normalised to the signal for 8 M urea. The standard deviation of the slope and intercept were 0.7 and 0.4, respectively, and the standard error was 0.408; five data points, each being the average of all voxel intensities contained within the image for that specific concentration of urea, were analysed. The coefficients of this equation are constant for a given set of experiments, and a function of both the relative number of scans required in the reference and sample images, and the tuning of the receiver coil.

Eq. (6) was then used to calculate the total content of urea in three-dimensional images of a pulse of urea passing through a column. Samples of 500 μl of 8, 6, 4 and 2 M urea were injected into the column. Three or four three-dimensional images of the urea pulse were then recorded as the pulse progressed through the column using the three-dimensional RARE IR pulse sequence. The total urea content measured from a given image was then calculated using Eq. (6). The results of these experiments are shown in Table 1, and confirm the quantitative nature of these measurements.

Table 1
Urea content measured for samples of the stated urea concentration using MR imaging, as determined from the average of three three-dimensional images

Sample	Total urea content (mmol)	MR imaging measurement (mmol)
8 M urea	4.0	3.9 ± 0.7
6 M urea	3.0	3.0 ± 0.6
4 M urea	2.0	1.6 ± 0.9
2 M urea	1.0	1.1 ± 0.6
8 M urea with lysozyme	4.0	3.9 ± 0.9

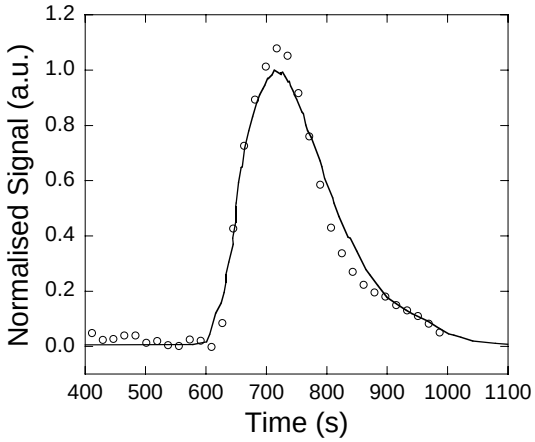

Fig. 2. Chromatograms of urea within a 5 ml HiTrap SEC desalting column; circles (○) represent MR data and the solid line (—) represents data from a standard chromatogram. The time stated is the time after injection of the urea sample. The chromatographic elution profile was shifted in time to account for the extra length of tubing between the valve and the column used in the MR experiment, ignoring any diffusive effects. Both plots were normalised to the same area.

Further, validation of the quantitative nature of the MR measurement of the urea pulse was achieved by comparing the urea concentration leaving the column as a function of time, as determined by MR imaging, with the urea concentration measured using UV monitoring of the column eluate in standard FPLC. The standard chromatographic elution profiles were produced by spiking urea with DTT to produce a change in UV absorbance of the column eluate. Although DTT is a larger molecule than urea, it is much less than the molecular weight cut off for the column and therefore should behave in a similar manner to urea. An equivalent chromatogram was obtained using MR imaging by collecting a series of one-dimensional inversion recovery profiles of the column at 30-s intervals for 15 min and then plotting the signal intensity of the data point immediately before the exit of the column over the entire acquisition time. The resulting chromatograms are presented in Fig. 2. It can be seen that the profiles of each method match very well, and in fact the discrepancy could be entirely due to the reproducibility of any single sample of urea.

Fig. 3 shows two-dimensional slices extracted from a full three-dimensional image of a 0.5 ml sample of urea in the column approximately 6 min after injection. Fig. 3 shows that there is a significant tail down one wall of the column. Hence, in contrast to the chromatographic elution profiles, the two-dimensional images extracted from the three-dimensional dataset reveal the nature of the non-ideal behaviour and thus can provide insight into how the column design and packing medium can be optimised to improve the performance of chromatographic columns.

A disadvantage of the ^{1}H three-dimensional images is that they have a much longer acquisition time than two-dimensional images, i.e. of the order of 10 min rather than 30 s. Therefore, in order to obtain a more accurate representation of the temporal evolution of the urea samples, two-dimensional images were also taken and were calibrated in the same manner as the three-dimensional images. The concentration values calculated from the two-dimensional images were similar to those measured in the three-dimensional images. Fig. 4 shows a selection of images of a pulse of 8 M urea travelling down the column at different times. The distortion of the pulse due to the bulk motion of the urea during the acquisition time (the motion artefact) can be estimated from the superficial velocity. The superficial velocity is 0.041 mm s^{-1}, which suggests the urea sample moves ∼1.2 mm, which is equivalent to 4 pixels, during the acquisition time.

4.2. Direct imaging of unlabelled lysozyme

In this section a pulse sequence is described that enables quantitative imaging of unlabelled lysozyme. This sequence

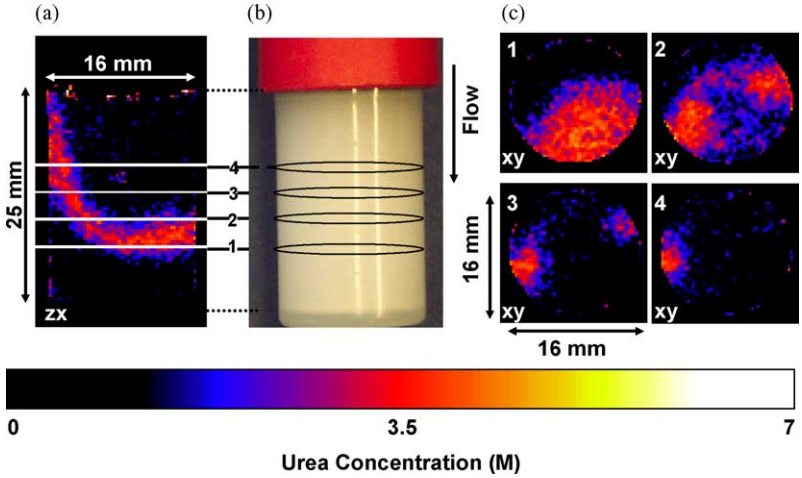

Fig. 3. (a) Two-dimensional *zx* slice taken from a three-dimensional RARE image of a 0.5 ml sample of urea. The image slice is taken along the length of the column. (b) shows a photograph of the column and the position at which four (1–4) *xy* image slices shown in (c) have been extracted from the three-dimensional image. Voxel resolution is 312 μm × 312 μm × 312 μm.

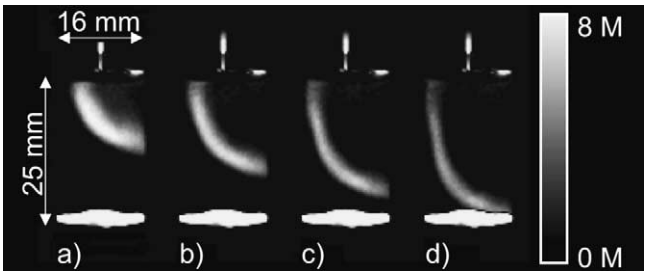

Fig. 4. Selected images from a series of two-dimensional images taken in rapid succession showing the temporal evolution of an 8 M urea sample as it travels down the column: (a) $t = 390$ s, (b) $t = 480$ s, (c) $t = 570$ s, and (d) $t = 660$ s. The grey scale gives the urea concentration (M). In-plane pixel resolution is 312 μm × 312 μm.

is first characterised and validated. The effect of lysozyme on the quantitation of urea concentration determined by the MR measurement described in the previous section is then investigated and finally the RF pulse sequences to image unlabelled urea and lysozyme are combined to image a lysozyme-urea separation using a 5 ml HiTrap column.

4.3. Quantitation of lysozyme profiles

Whilst the intensity of the ^{1}H signal received from lysozyme in the column is approximately three orders of magnitude less than the ^{1}H signal received from either the water or urea present in the sample, it is possible that lysozyme will alter the relaxation properties of water and urea in the near vicinity and hence alter the signal intensity of these species in the images. This hypothesis was tested by measuring the T_1 and T_2 relaxation time constants for water and urea in the column in the presence and absence of lysozyme. To assess the effect of lysozyme on T_1 and T_2, a high concentration of lysozyme was used (25 mg ml^{-1}), which approaches the upper limit which would be present in the column (70 mg ml^{-1}). The results are presented in Table 2.

The increase in T_2 relaxation time constant for water in the presence of 25 mg ml^{-1} lysozyme, both with and without urea, is approximately 20% (Table 2). In this work, this effect is utilised to obtain images of the lysozyme distribution within a HiTrap desalting column, without resorting to labelling of the protein. The T_2 relaxation time constant determines the intensity of detectable signal remaining after an excitation (see Eq. (1)). Consequently, by using a pulse sequence that initially excites the nuclear spins and then has an appropriate delay before reading the signal, it is possible to create a sequence that is sensitive to the lysozyme concentration, as shown in Fig. 1. The change in T_2 is relatively small (38 ms versus 49 ms) and therefore only one-dimensional profiles were acquired to ensure sufficient signal-to-noise and temporal resolution in the acquired data.

Table 2
Relaxation time constants for water and urea in various lysozyme and urea solutions in the HiTrap column

Sample	T_1 (s)		T_2 (ms)	
	Water	Urea	Water	Urea
Water	1.469	–	38	–
25 mg ml^{-1} lysozyme	1.378	–	49	–
8 M urea	1.001	0.868	33	52
8 M urea with 25 mg ml^{-1} lysozyme	0.976	0.873	48	50

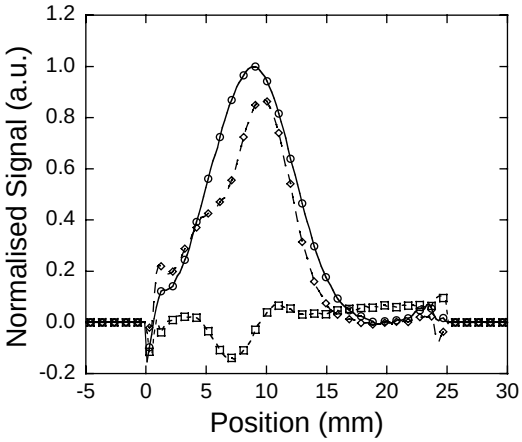

Fig. 5. Normalised ^{1}H intensity profiles within a HiTrap column taken with T_2 weighting, and summing the first 16 echoes. Profiles are shown following injection of 0.5 ml of 25 mg ml^{-1} lysozyme (○), 8 M urea (□), and a mixture of 25 mg ml^{-1} lysozyme and 8 M urea (◇).

Fig. 5 shows three signal intensity profiles recorded along the length of the column taken at the same time after injection for samples of lysozyme, lysozyme and urea, and urea only. In each case, the profile shown is the difference between a reference profile obtained with only phosphate buffer in the column and the profile obtained with the stated sample. The two profiles containing lysozyme clearly show an increase in signal over the column equilibrated with phosphate buffer, whereas the third profile, for a pulse of urea only, does not show evidence of any pulse but does show a maximum (negative) deviation from the baseline of 0.1.

Although the above experiments demonstrate the selectivity of the sequence to lysozyme imaging, they do not prove that the pulse sequence produces a quantitative measurement. To test the quantitative nature of the sequence a series of samples of lysozyme were injected with concentrations in the range 5–25 mg ml^{-1}, and the procedure described earlier for quantitation of urea pulses was repeated. A linear fit to the integral of the signal intensity against the sample concentration was calculated and is described by Eq. (7):

$$[\text{Lys}] = 358S + 0.13, \quad (7)$$

where [Lys] is the lysozyme concentration in mg ml^{-1} and S is the signal intensity. The standard deviation of the slope and intercept were 9.3 and 0.03, respectively, and the standard error was 0.51; 56 data points were analysed.

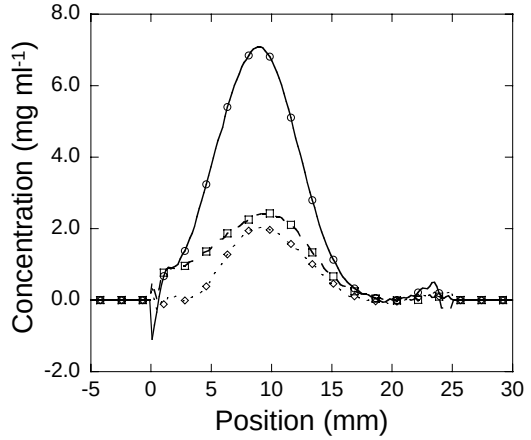

Fig. 6. Twenty-five mg ml^{-1} (○), 10 mg ml^{-1} (□), and 7.5 mg ml^{-1} (◇) lysozyme profiles recorded 130 s after injection of a 0.5 ml pulse. The horizontal axis shows the position along the column (in mm); the entrance to the column is at 0 mm.

Fig. 6 shows three pulses of 7.5, 10 and 25 mg ml^{-1} lysozyme acquired 130 s after injection. The concentration shown in Fig. 6 is the overall concentration in each pixel, as calculated from Eq. (7), and includes the volume of liquid contained within the pores of the packing—this intra-particle space does not contain lysozyme. Thus, the actual local concentration of lysozyme in the inter-particle space will be much larger than that reported in Fig. 6. The void volume of the column is 1.5 ml, which suggests that the peak local concentration in the inter-particle space could be as much as 24 mg ml^{-1}.

Fig. 7 shows the evolution of the elution profile with time for a sample of 25 mg ml^{-1} lysozyme in the column. Each profile represents the elution profile that would be observed if the column were the length specified for that profile. The area under each peak, which is proportional to the estimated total quantity of lysozyme in the column, is constant to within ±7% for all four elution profiles.

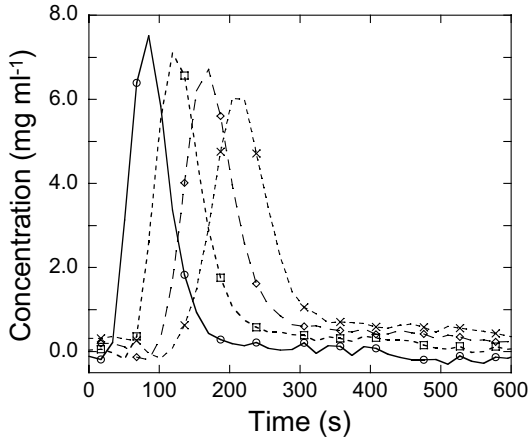

Fig. 7. MR elution profiles for a sample of 25 mg ml^{-1} lysozyme on a 5 ml HiTrap desalting column at 5 mm (○), 10 mm (□), 15 mm (◇) and 20 mm (×) from the entrance to the column. Each curve shown is comprised of 40 data points evenly distributed over the total acquisition time.

4.4. Effect of lysozyme on urea imaging

The introduction of lysozyme to the urea sample entering the column could influence the signal intensity associated with urea and hence reduce the accuracy of the calibration equation given earlier for urea measurements (Eq. (6)). As noted above, the major influence lysozyme will have on the urea signal intensity is through the changes in the relaxation properties of nearby water and urea molecules (see Table 2). The T_1 relaxation time constant for both water and urea in the presence of lysozyme is relatively constant (2.5% lower in the presence of lysozyme). However, the T_1 relaxation time constant for water in phosphate buffer decreases by 0.1 s or approximately 10% in the presence of lysozyme. This suggests that a small amount of signal could be detected from the lysozyme in solution when using the inversion pulse sequence, even if there is no urea present. This could lead to an increase in total observed signal for the 25 mg ml^{-1} lysozyme in 0 M urea sample by as much as 10% of that observed for the 8 M urea sample. In reality, the error will be less than this due to the further dilution of the lysozyme upon entering the column and the dominating effect of urea in the mixture since lysozyme is present in much lower quantities.

The presence of lysozyme also increases the T_2 of the surrounding water molecules. RARE imaging sequences are inherently T_2 weighted and consequently this could further influence the observed signal. The effective T_2 weighting in a RARE image will be approximately equal to the attenuation at the midpoint of each echo train, that is, after eight echoes [15,16]. For the above imaging sequence, this equates to approximately 20 ms, which could produce a further enhancement of the total image intensity by as much as 10%.

To test the effect of adding lysozyme to urea, a three-dimensional RARE IR image was acquired from a 0.5 ml pulse of 8 M urea containing 50 mg ml^{-1} lysozyme. This is the near the upper limit for effective separation (70 mg ml^{-1}) and represents a worst case scenario regarding the influence of lysozyme on data quantitation. It was found that the total urea content in the images was calculated to be 3.9 ± 0.9 mmol, in excellent agreement with the known amount injected of 4 mmol. Therefore, it is concluded that although the lysozyme may influence the signal intensity, the effect is not significant and quantitative images of urea are still obtained.

4.5. Imaging of a desalting process

Alternate one-dimensional profiles using the inversion recovery (for urea imaging) and T_2 weighted (for lysozyme imaging) pulse sequences were taken for a sample of 0.5 ml 8 M urea containing 25 mg ml^{-1} lysozyme. These profiles were collated to produce a real time image of the separation of urea from unlabelled lysozyme in a 5 ml HiTrap desalting

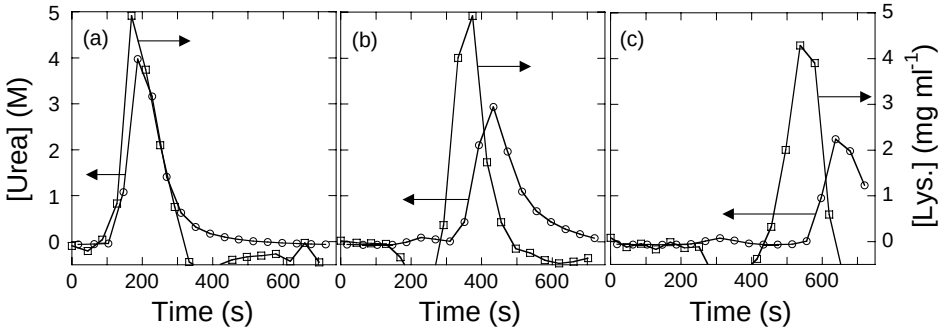

Fig. 8. Lysozyme (□), and urea (○) concentrations at distances of (a) 2; (b) 12 and; (c) 22 mm from the entrance to the column. The lysozyme concentrations quoted are the values of overall lysozyme concentration within each pixel. As discussed in the text, since lysozyme does not enter the intra-particle space of the packing medium, the concentration of lysozyme in the inter-particle space of the column will be higher than these values.

column. Fig. 8 shows the variation in urea and lysozyme concentration at three positions in a column; 2, 12 and 22 mm from the entrance. No data are shown for the region immediately above the exit of the column due to the presence of the outlet frit which influences the relaxation times observed in this region, and hence spurious concentration profiles are obtained.

The separation shown in Fig. 8 is not as complete as that claimed by the manufacturer, even if extrapolated to the full column length. The dilution factor for the sample is about 4, compared to the dilution factor quoted by the manufacturer of 3, while the urea remaining at 95% protein recovery is about 10%. Further, the trailing edge of each sample band is not as sharp as the elution profile demonstrated by the manufacturer. However, a large number of runs were performed with the same column so this could be due to fouling in the entrance to the column or due to the higher viscosity of the urea and lysozyme sample used in this work compared to the 2 mg ml^{-1} BSA and 0.5 M NaCl sample demonstrated by the manufacturer.

The MR methodology described here permits quantitative visualisation of the individual components of the separation and also allows us to measure directly the characteristics of the separation necessary to model the mass transfer processes inside the column. Further, the techniques developed here will permit easier quantification of any non-ideal behaviour observed in chromatographic elution profiles. These two features should enable researchers to more accurately develop mathematical models appropriate to the real experimental conditions and hence improve the predictive power of such models.

5. Conclusions

An MR imaging technique has been implemented for the quantitative measurement of both urea and lysozyme within a HiTrap desalting column. These measurements are achieved without incorporation of image contrast agents into the system, and are shown to give an absolute measure of concentration to within 15%, given the known amount of the species injected at the top of the column. Further, quantitative agreement is observed between the MR concentration profile for an 8 M urea sample with an elution profile obtained by traditional UV chromatography analysis of an 8 M urea sample doped with DTT.

In addition to imaging the lysozyme and urea as single-component systems within the column, time-resolved, quantitative concentration profiles of both species were acquired during a desalting process. This was achieved by alternating urea and lysozyme imaging sequences such that concentration profiles of each species were achieved with a temporal resolution of 30 s.

The ability to use MR imaging to study, quantitatively, urea and protein without introducing contrast agents into the system, which may alter protein behaviour as well as make quantitation difficult, offers new opportunities to assess the effect of packing and operating conditions on process performance. Further, by obtaining molecule-specific concentration profiles within the column in real-time, it is possible to make objective judgements on how best to model the separation process. Once a model is chosen, it is then possible to use transport parameters (e.g. diffusion coefficients) measured directly on the system of interest and, of course, to test the performance of any model against the detailed image data acquired. This is the subject of ongoing work.

References

[1] E.J. Fernandez, C.A. Grotegut, G.W. Braun, K.J. Kirschner, Phys. Fluids 7 (1995) 468.
[2] L.D. Plante, P.M. Romano, E.J. Fernandez, Chem. Eng. Sci. 49 (1994) 2229.
[3] U. Tallarek, E. Baumeister, K. Albert, E. Bayer, G. Guiochon, J. Chromatogr. A 696 (1995) 1.
[4] N.S. Mitchell, L. Hagel, E.J. Fernandez, J. Chromatogr. A 779 (1997) 73.
[5] M.H. Werner, G.M. Clore, A.M. Gronenborn, A. Kondoh, R. Fisher, FEBS Lett. 345 (1994) 125.
[6] B. Batas, J.B. Chaudhuri, Biotechnol. Bioeng. 50 (1996) 16.
[7] M.M. Lyles, H.F. Gilbert, Biochemistry 30 (1991) 613.

[8] H. Lanckriet, A.P.J. Middelberg, J. Chromatogr. A 1022 (2004) 103.
[9] Y. Maeda, H. Koga, H. Yamada, T. Ueda, T. Imoto, Protein Eng. 8 (1995) 201.
[10] S.M. West, J.B. Chaudhuri, J.A. Howell, Biotechnol. Bioeng. 57 (1998) 590.
[11] P.T. Callaghan, Principles of Nuclear Magnetic Resonance Microscopy, Clarendon Press, Oxford, 1991.
[12] L.F. Gladden, Chem. Eng. Sci. 49 (1994) 3339.
[13] E.L. Hahn, Phys. Rev. 80 (1950) 580.
[14] H.Y. Carr, E.M. Purcell, Phys. Rev. 94 (1954) 630.
[15] J. Hennig, A. Nauerth, H. Friedburgh, Magn. Reson. Med. 3 (1986) 823.
[16] A.J. Sederman, M.D. Mantle, L.F. Gladden, J. Magn. Reson. 161 (2003) 15.